

# Flows Through Sequential Orifices With Heated Spacer-Reservoirs

R. C. Hendricks and T. Trent Stetz  
*Lewis Research Center*  
*Cleveland, Ohio*

Prepared for the  
Ninth International Cryogenics Engineering Conference/  
International Cryogenic Materials Conference  
Kobe, Japan, May 11-14, 1982



# FLOWS THROUGH SEQUENTIAL ORIFICES WITH HEATED SPACER-RESERVOIRS\*

R. C. Hendricks and T. Trent Stetz†

National Aeronautics and Space Administration  
Lewis Research Center  
Cleveland, Ohio

## INTRODUCTION

The principal use of sequential inlets in power systems is in fluid control. Turbomachines have several sequential inlets such as seals, vane rotors, bearings, etc., and in many cases the flows are choked. The downstream inlet is usually treated independently of the upstream configuration. As machines become more compact and the power density is increased, the effects that sequential inlets can produce on the flow field and subsequent engine performance become significant. On several occasions the failure, or derating, of high-performance turbomachinery has been attributed to instabilities excited by fluid flow through the seals or blade vanes (ref. 1).

In an effort to understand a flow separation phenomenon observed in a multiple-step seal configuration, studies were made in single-inlet tubes and multiple-inlet geometries. In choked flows through single-inlet tubes a jetting phenomenon was found to a length-diameter ratio  $L/D$  of 105 over a range in fluid temperatures and pressures in both simple and complex geometries. Jetting has also been found in multiple-step seals (refs. 2 to 5). Flows through sequential inlets represent a complex problem, and theory for such flows is not well developed. For example, the flow field can be rotating, have multiple-vortex formations, and have multiple separations and variable properties with a variety of surface boundary conditions. Consequently an empirical relation to define regions of jetting in single inlets was advanced (refs. 2 and 3). Moreover, jetting was observed for choked flows in multiple-inlet configurations for small  $L/D$  spacings, where the flow rate for  $N$  sequential inlets is essentially that of a single inlet. For large  $L/D$  spacings the flow follows a simple power-law relation based on the flow through a single inlet, and the exponent is nearly constant outside the thermodynamic critical region (ref. 5).

The pressure profiles for single and multiple inlets are more complex and are not relatable in such simple terms. For one range of flow and  $L/D$  conditions the profiles resemble conventional parabolic pressure drops for flow through a tube, and for another range of flow and  $L/D$  conditions the profiles monotonically increase with axial position, resembling the profile of a supersonic diffuser.

Most systems with sequential inlets involve heat and mass transfer to some degree, but the cited studies have been carried out either under adiabatic or near adiabatic conditions. The purpose of this paper is to investigate some effects of heating in the zones between sequential inlets. The study will present results for mass flux, report typical pressure and temperature profiles, compare the Nusselt number ratios, and describe "burnout"

---

\*A shortened version of this report was prepared for the Ninth International Cryogenics Engineering Conference/International Cryogenic Materials Conference, Kobe, Japan, May 11-14, 1982.

†Current address, Miami University, Oxford, Ohio.

for sequential inlets with heated spacer-reservoirs. It will be shown that near adiabatic conditions do not materially affect the flow or pressure profiles, but diabatic conditions (constant heat flux) can lead to significant flow reductions and ultimately burnout or catastrophic failures.

## ANALYSIS

As the theory for flows through sequential inlets is not well developed, previous success using a combined thermodynamic and choked flow analysis will be applied here (ref. 5). The process at the  $i^{\text{th}}$  inlet (fig. 1) is assumed to expand isentropically through that inlet, followed by isobaric recovery in the spacer-reservoir with (or without) heat addition. The governing equations for the  $i^{\text{th}}$  inlet become

$$\left(\frac{G}{C_f}\right)_i^2 = 2\rho_i^2(H_o - H_i) \quad (1)$$

where the constraints are

Isentropic

$$S_o(P_o, T_o)_i = S(P_e, T_e)_i$$

Isobaric

$$P_{e,i} = P_{o,i+1}$$

(2a)

Critical choked flow

$$G_m^2 \left(\frac{dV}{dP}\right)_{e,(i=N)} = -1 \quad (2b)$$

where

$$G_m^2 = \left(\frac{2}{V^2}\right) \int_P^{P_o} V \, dP \quad (i = N)$$

Upon convergence,  $(G/C_f)$  approaches  $G_m$ , with  $C_f = 0.75$ . Fluid properties were calculated by using GASP (ref. 6).

The solution is complicated because the pressure ratios across each inlet are unknown, and the stability of the solution is not guaranteed. Thus to solve the problem (fig. 1), one must determine the inlet stagnation conditions, assume a pressure ratio for the first inlet, calculate the conditions of the expansion, and then determine the stagnation conditions for the next inlet (including heat addition or extraction in the spacer-reservoir). Repeat these steps for the next  $N - 1$  inlets. At the  $N^{\text{th}}$  inlet, determine the expansion conditions and compare them to those calculated from

the choked-flow constraint. If the flow rates and pressure ratios are within a convergence range, the flow rates and pressure ratios are said to be computed for the prescribed inlet and any addition of heat into (or out of) the sequential inlets. In essence, the constraints form the basis of a variational approach where we determine a solution with the least increase in entropy, with real fluid properties determined by using the code GASP (ref. 6).

For a gas the governing equations can be approximated by using the isentropic expansion conditions and the perfect-gas equation of state as done by Komotori and Mori (ref. 7) and others. The flow rate for the  $i^{\text{th}}$  inlet becomes

$$G_{i+1}^2 = \frac{2\gamma P_i \rho_i}{\gamma - 1} \left( x^{2/\gamma} - x^{(\gamma-1)/\gamma} \right) \quad (3a)$$

where

$$x = \frac{P_{i+1}}{P_i} \quad (3b)$$

and the constraints of equations (2a) and (2b), still apply. Over the range of gaseous conditions investigated, the solutions of equations (2) and (3a) are in good agreement. Thus the simpler approach, equation (3a), can be used for near constant property gases but not for variable fluid property conditions as will be shown later.

As the flow through such systems is not well understood, it follows that even less understanding exists for heat transfer. In this paper, the heat transfer results will be compared by using the relation:

$$Nu_r = 1 - \frac{\partial \ln \rho}{\partial T} (T_w - T_b) = (1 + \beta \Delta T) \quad (4)$$

Here  $Nu_r$  represents the ratio of experimental to calculated Nusselt numbers, and all the property parameters are evaluated at bulk conditions. The calculated Nusselt number is that of McAdams, but others such as the Petukhov formulation are equally valid (ref. 8).

#### APPARATUS AND INSTRUMENTATION

The flow system is essentially that described in references 4 and 9, with modifications to accommodate individually heated spacer-reservoirs. The test installation is shown in figure 2. A more detailed description of the test configuration is given in figure 3. The spacer-reservoir and orifices were made of stainless steel, sandwiched together between end flanges, held together by rods, sealed with flat Mylar gaskets, and electrically isolated from ground. The wall thermocouples (Chromel-Alumel) were swaged in tubes that were in turn attached to the inner surface through a hole in the spacer-reservoir tube. The bulk temperature thermocouples were of the same swaged construction but were inserted at the centerline of the spacer-reservoir. In addition to the five wall and five bulk thermocouples in each spacer-reservoir, there were five static pressure taps per spacer and one

pressure tap in the center of each orifice. In addition, inlet and outlet pressures and temperatures were measured. Copper bus flanges were clamped onto the spacer-reservoirs, and the power was supplied from either an ac or dc source to one of the three spacer-reservoirs. The overall system sensitivity was not sufficient to determine any difference between using ac or dc power. The working fluid was nitrogen, and the data range included liquid and gas for reduced inlet stagnation pressures up to 2 ( $P_{r,0} = 2$ ).

Motion pictures were used to record the tests run to simulate burnout conditions. Although the seals failed and pressure "bulged" the spacers, some good data were obtained.

## RESULTS AND DISCUSSION

In this section, a comparison is made between theoretical predictions and experimental findings of mass flux, pressure and temperature profiles, heat transfer, and burnout.

### Mass Flux

The theoretical analysis predicts a decrease in flow rate with the addition of heat into the spacer-reservoir. Heat addition in the first spacer (inlet) adjacent to the inlet orifice is most effective in reducing the flow rate; heat addition in the last spacer-reservoir (outlet) is least effective.

Now defining the flow coefficient as the ratio of experimental or calculated mass flux with the  $j^{\text{th}}$  spacer-reservoir heated to that without heating, viz,

$$C_f = \frac{G_j}{G_0} \quad (5)$$

and applying this definition to the gaseous nitrogen data provide the curves of figures 4(a) to (c). These figures present a comparison between theory and experiment. The experimental data are slightly above but in reasonable agreement with theory. Knowing that for gases the primary variable in equation (5) is density, the bulk temperature can be used to approximate changes in the flow coefficient:

$$C_f = \frac{G_j}{G_0} \sim \sqrt{\frac{T_{b,0}}{T_{b,j}}} \quad (6)$$

Thus a check can be made by using the bulk temperature rise. The results show the data below, but also in reasonable agreement with, theory for the accuracy of this experiment.

The liquid-nitrogen data (figs. 4(d) to (f)) exhibit the proper general trends but are significantly higher than theory for each spacer-reservoir. Although the simplicity of the theory and the experimental errors each contribute to the disagreement, a change in fluid model similar to that for film boiling of cryogenics (ref. 9) is speculated to be most significant. It appears that fluid jetting or carryover from one spacer-reservoir to another is increased as heating is increased. Thus the assumption of a constant flow coefficient, which was satisfactory for sequential inlets without heat-

ing, is no longer valid<sup>1</sup>. More data and analyses are required before the flow coefficients can be varied with any confidence.

### Pressure Profiles

Typical axial pressure distributions are given for gaseous and liquid nitrogen for three heat inputs in figure 5. Because the pressure profiles for gaseous nitrogen with and without heating were similar for the heat input range of this experiment, only one profile is shown. The pressure profiles for liquid nitrogen were also somewhat similar, but near the outlet a significant shift from jetting to gas-like behavior was noted; also the stage pressure ratio decreased and the pressure level increased as heating increased. A similar trend is predicted by the theory. The flattening of the profiles with increased heating is characteristic of a liquid coring model (jetting or carryover). The change in the model was previously suggested as a possible reason for departure from theory (refs. 2 and 3).

### Temperature Profiles

Although some of the thermocouples failed, enough remained to define wall and bulk temperature profiles for both the liquid and gaseous cases. The inlet spacer-reservoir temperature profiles (fig. 6) are typical. The inlet was hotter because of the vortex zone; the central part was cooler because the diverging jet tended to wash the wall; and with sufficient heat input the outlet could easily reach burnout temperatures because of the stagnation zone ahead of the last orifice inlet. The centerline bulk temperatures responded to the heat input but were not sufficiently accurate to indicate completeness of mixing in the heated section; downstream the wall and bulk temperatures usually ran within a degree of one another, indicating good mixing.

### Heat Transfer Comparisons

The analysis of flow in tubes was extended to spacer-reservoirs of sequential inlets, and it is not surprising that the agreement with experimental data was poor, as shown in figure 7 by the departure of the Nusselt number from unity. A lack of knowledge of the proper hydraulic diameter (herein the spacer-reservoir) and the flow patterns to be used leaves too many uncertainties. It is apparent that more work needs to be done in order to understand both the flow patterns and the heat transfer characteristics.

### Burnout

Each spacer-reservoir was heated to near burnout, a condition defined by a 4- to 7-cm section coming to a orange-red glow. From another source, this coloration of stainless steel indicates an optical pyrometer temperature of 1400° to 1600° F. The surface temperature was estimated at 1100° to 1300° F when heat input is less than 50 J/g. The pressure (1 MPa) was

---

<sup>1</sup>Although the data could be matched by forcing the flow coefficient ( $C_f = C_f(\Delta H)$ ; e.g., 0.84 for  $\Delta H = 10$ ), the experimental data are not sufficient to draw any general conclusions at this time.

sufficient to bulge the spacer-reservoir, and the system was shut down before it achieved fully developed burnout conditions. The decrease in flow rate was dramatic and physical destruction appeared imminent.

In subsequent tests with liquid nitrogen, motion pictures were taken as the system was cycled between the adiabatic and diabatic conditions. The heat input was varied incrementally until conditions approached burnout, where power was then held constant. The time-temperature conditions could be visualized by watching the frost melt, the water boil, and the surface dry out. The advancement of the front began near the inlet of the  $(N + 1)^{\text{th}}$  orifice (bottom of the picture) and continued to move back upstream until equilibrium was achieved. If the heat input was large enough to produce a reduction in flow, the available cooling decreased and for a constant heat flux the surface temperature continued to increase until equilibrium or physical destruction was achieved. In this case, a section of the tube began to glow orange-red. The glowing section expanded and, in our case, when a pseudo-equilibrium was achieved, the power was shut off. As shown in the motion pictures, profuse leakage of coolant past the seals can occur under these extremes and could contribute to the loss of available coolant and to the subsequent rise in surface temperature. When the system was allowed to approach equilibrium, the flow was decreased but not stopped, even though over two-thirds of the spacer-reservoir length was orange-red. Repeating the cycle did not appear to change these observations.

The motion picture supplement is available from the NASA Lewis Research Center Photographic and Printing Branch.

#### SUMMARY OF RESULTS

Theoretical and experimental results for the flow of fluid nitrogen through a four-sequential-orifice configuration shows that heat addition in the first spacer-reservoir adjacent to the inlet orifice is most effective in reducing the flow rate and that heat addition in the last spacer-reservoir is least effective. The differences are readily measurable for the gaseous case but are within the scatter of the data for the liquid case.

The measured mass fluxes for the gas were in reasonable agreement with theory. The measured mass fluxes for the liquid nitrogen were significantly higher than predicted even though the trends were correct, indicating that a nonconstant flow coefficient must be used in the analysis. The carryover or jetting appeared to be significantly influenced by heating.

The pressure profiles were similar for various heat inputs, with the liquid profiles altered more. Pressure ratio and level increased with heat input. (A ratio of unity represents no flow loss.) The major flow loss shifts toward the exit orifice.

The wall and bulk temperature profiles responded directly to heat input, and "burnout" in the downstream portion of the spacer-reservoir was readily achieved. A comparison to tube heat transfer correlation was not successful. A motion picture was taken to illustrate the cooldown and burnout cycle (orange-red color over most of the tube). For a near equilibrium state ( $P_{r,0} = 1 \text{ MPa}$ ;  $T_{r,0} = 89 \text{ K}$ ), burnout of the tube significantly decreased, but did not stop the flow. The motion picture is available from the NASA Lewis Research Center Photographic and Printing Branch.

## APPENDIX - SYMBOLS

b	exponent
$C_f$	flow coefficient
D	diameter of spacer-reservoir
d	diameter of inlet
G	mass flow rate, $\rho u$
$G^*$	flow-normalizing parameter, 6010 g/cm <sup>2</sup> -s for nitrogen
H	enthalpy
L	length of separation
l	length of orifice
N	number of inlets
P	pressure
S	entropy
T	temperature
u	velocity
V	specific volume
X	pressure ratio
Z	compressibility
$\beta$	volumetric expansion factor, $(\partial \ln \rho / \partial T)_p$
$\rho$	density, 1/V

### Subscripts:

b	bulk
c	thermodynamic critical
e	exit
I	isentropic
i,M,N	i <sup>th</sup> , M <sup>th</sup> , N <sup>th</sup> sequential inlet
j	j <sup>th</sup> spacer heated
m	maximum
o	stagnation, or no spacer heated
r	reduced by normalizing parameter
1	case for N = 1, the single inlet, or unit

## REFERENCES

- 1 Rotordynamic Instability Problems in High-Performance Turbomachinery, NASA CP-2133, 1980.
- 2 Hendricks, R. C.: Some Aspects of Free Jet Phenomena to 105 L/D in a Constant Area Duct. Proc. of 15th Int. Congress on Refrigeration, Int. Inst. of Refrigeration, Paris, France, 1979, Paper B1-78.
- 3 Hendricks, R. C.: Free Jet Phenomena in a 90-Degree Sharp Edge Inlet Geometry. Advances in Cryogenic Engineering, Vol. 26, K. D. Timmerhaus, ed., 1979, Paper CC7.
- 4 Hendricks, R. C.; and Stetz, T. T. : Flow Through Axially Aligned Sequential Apertures of the Orifice and Borda Types. Presented at 20th ASME-AIChE Nat. Heat Transfer Conf., Milwaukee, Wis., Aug. 1981, Paper ASME 81-HT-79.
- 5 Hendricks, R. C.; and Stetz, T. T. : Experiments on Flow Through One to Four Inlets of the Orifice and Borda Types. Proc. of Cryogenic Engr. Conf./Int. Cryogenic Materials Conf., San Diego, Calif., Aug. 1981, Paper JB-7.



- 6 Hendricks, R. C.; Baron, A. K.; and Peller, I. C.: GASP - A Computer Code for Calculating the Thermodynamic and Transport Properties for Ten Fluids: Parahydrogen, Helium, Neon, Methane, Nitrogen, Carbon Monoxide, Oxygen, Fluorine, Argon, and Carbon Dioxide. NASA TN D-7808, 1975.
- 7 Komotori, Kazunari; and Mori, Hideo: Leakage Characteristics of Labyrinth Seals. Proc. of 5th Int. Conf. on Fluid Sealing, Coventry, England, Mar. 30 - April 2, 1971. British Hydromechanics Research Association. Paper E4, pp. E4-45, E4-63.
- 8 Hendricks, R. C.; Yeroshenko, V. M.; Yaskin, L. A.; and Starostin, D. D.: Bulk Expansion Factors and Density Fluctuations in Heat and Mass Transfer. Proc. of 15th Int. Congress on Refrigeration, Int. Inst. of Refrigeration, Paris, France, 1979, Paper B1-119.
- 9 Hendricks, R. C.; Graham, R. W.; Hsu, Y. Y.; and Friedman, R.: Experimental Heat-Transfer Results for Cryogenic Hydrogen Flowing in Tubes at Subcritical and Supercritical Pressures to 800 Pounds Per Square Inch Absolute. NASA TN D-3095, 1966.

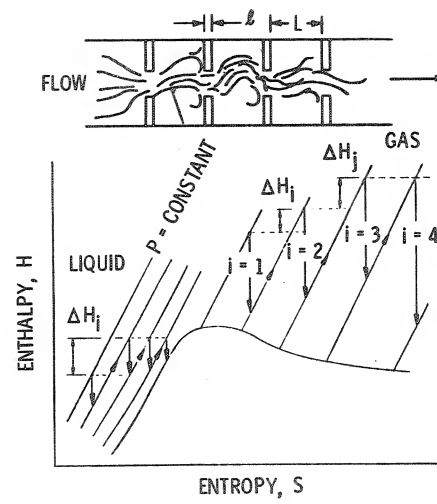


Figure 1. - Schematic H-S diagram for N sequential inlet expansions with heat addition.

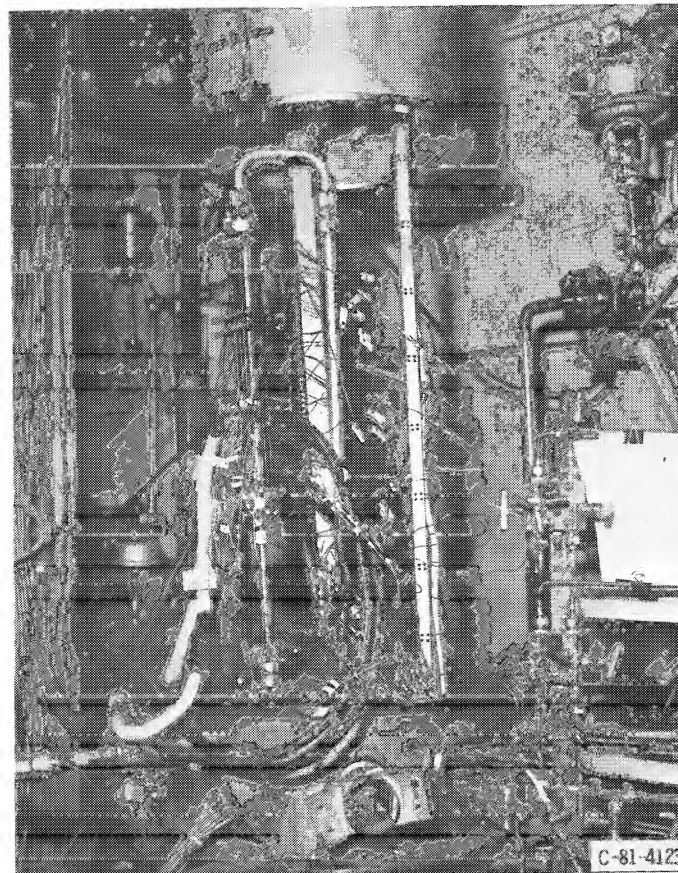


Figure 2. - Four-sequential-inlet configuration and experimental apparatus.

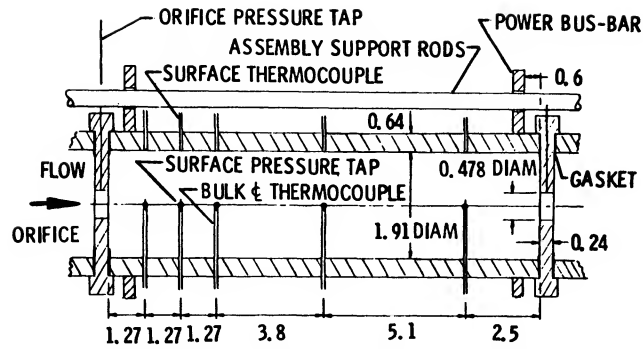


Figure 3. - Schematic diagram for an individual reservoir spacer-orifice inlet of an N-sequential-orifice-inlet test section. (Dimensions are in centimeters.)

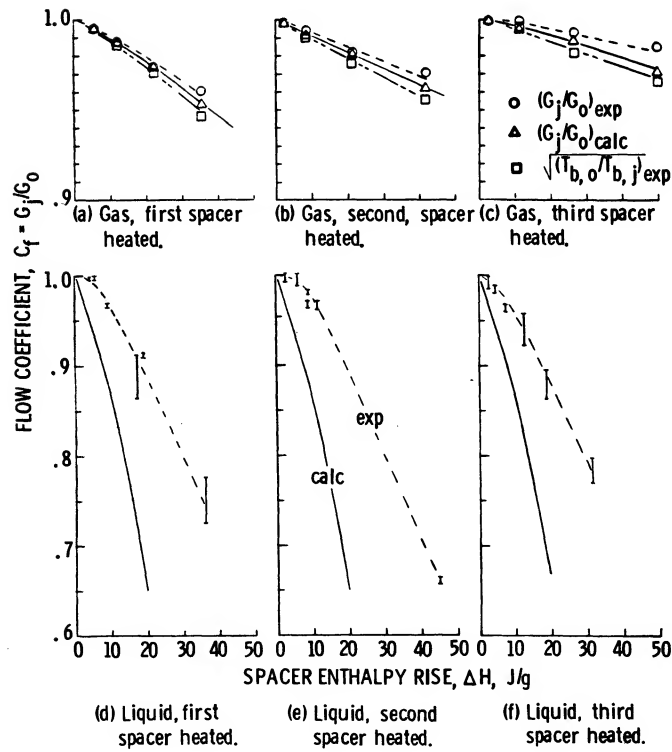


Figure 4. - Reduced mass flux as a function of reduced inlet stagnation pressure - comparison of theory with gaseous and liquid results.

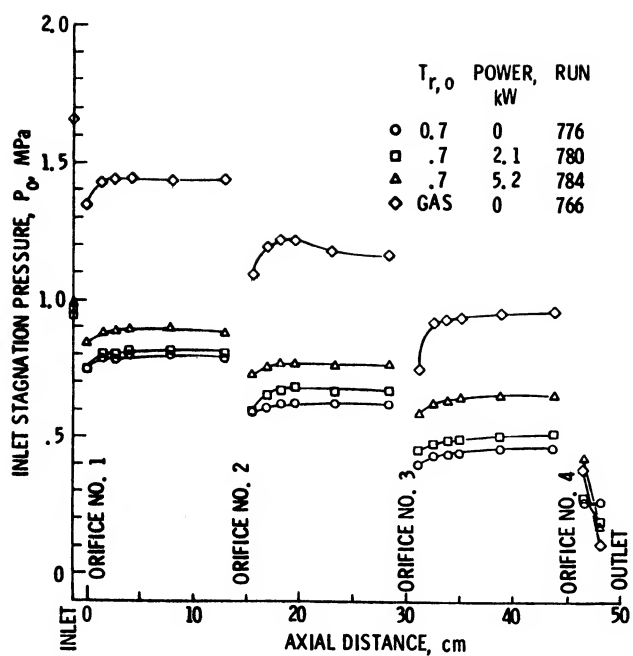


Figure 5. - Pressure profiles at selected heat inputs with first spacer heated.

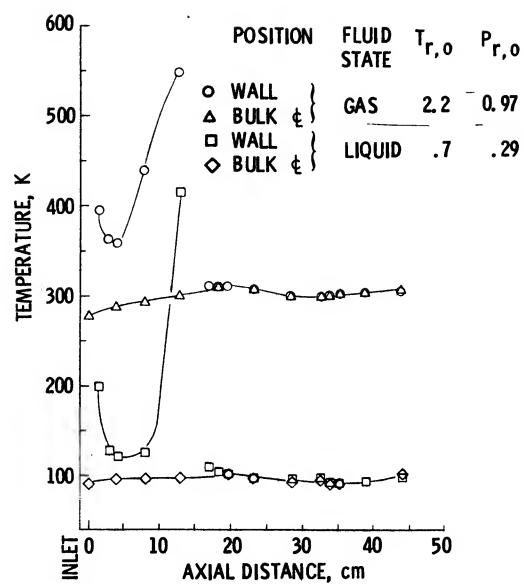


Figure 6. - Temperature profiles at selected heat inputs, first spacer heated.

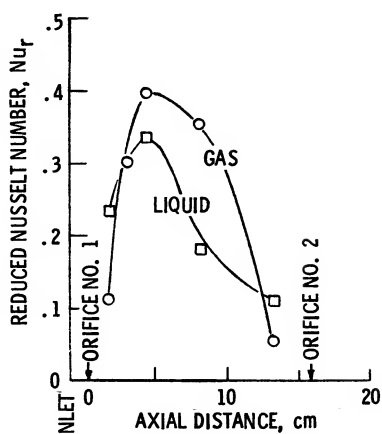


Figure 7. - Variation of reduced Nusselt number with axial distance, first spacer heated.

1. Report No. NASA TM-82855		2. Government Accession No.		3. Recipient's Catalog No.	
4. Title and Subtitle FLOWS THROUGH SEQUENTIAL ORIFICES WITH HEATED SPACER-RESERVOIRS				5. Report Date	
				6. Performing Organization Code 505-32-42	
7. Author(s) R. C. Hendricks and T. Trent Stetz				8. Performing Organization Report No. E-1224	
				10. Work Unit No.	
9. Performing Organization Name and Address National Aeronautics and Space Administration Lewis Research Center Cleveland, Ohio 44135				11. Contract or Grant No.	
				13. Type of Report and Period Covered Technical Memorandum	
12. Sponsoring Agency Name and Address National Aeronautics and Space Administration Washington, D.C. 20546				14. Sponsoring Agency Code	
15. Supplementary Notes A shortened version was prepared for the Ninth International Cryogenics Engineering Conference/ International Cryogenic Materials Conference, Kobe, Japan, May 11-14, 1982.					
16. Abstract Flow rates and pressure and thermal profiles for two-phase choked flows of fluid nitrogen were studied theoretically and experimentally in a four-sequential-orifice configuration. Both theory and experimental evidence demonstrate that heat addition in the first spacer-reservoir adjacent to the inlet orifice is most effective in reducing the flow rate and that heat addition in the last spacer-reservoir is least effective. The flows are choked at the exit orifice for large spacings and at the inlet orifice for small spacings. The moderate addition of heat available for this experiment did not materially alter this result for large spacings; however, significant heat addition for the small spacings tended to shift the choke point to the exit orifice. Nitrogen is used as the working fluid over a range of states from liquid to gas with a reduced inlet stagnation pressure range to $P_{r,o} = 2$ .					
17. Key Words (Suggested by Author(s)) Fluid mechanics Heat transfer Cryogenics			18. Distribution Statement Unclassified - unlimited STAR Category 34		
19. Security Classif. (of this report) Unclassified		20. Security Classif. (of this page) Unclassified		21. No. of Pages	
				22. Price*	